Chapter 7

Plasmonic Thin Film Solar Cells

Qiuping Huang , Xiang Hu , Zhengping Fu and Yalin Lu

Additional information is available at the end of the chapter

http://dx.doi.org/10.5772/65388

Abstract

Thin film solar cell technology represents an alternative way to effectively solve the world's increasing energy shortage problem. Light trapping is of critical importance. Surface plasmons (SPs), including both localized surface plasmons (LSPs) excited in the metallic nanoparticles and surface plasmon polaritons (SPPs) propagating at the metal/semiconductor interfaces, have been so far extensively investigated with great interests in designing thin film solar cells. In this chapter, plasmonic structures to improve the performance of thin film solar cell are reviewed according to their positions of the nanostructures, which can be divided into at least three ways: directly on top of thin film solar cell, embedded at the bottom or middle of the optical absorber layer, and hybrid of metallic nanostructures with nanowire of optical absorber layer.

Keywords: thin film solar cells, light trapping, localized surface plasmons (LSPs), surface plasmon polaritons (SPPs), light absorption enhancement

1. Introduction

Photovoltaic technology, the conversion of solar energy to electricity, can help to solve the energy crisis and reduce the environmental problems induced by the fossil fuels. Worldwide photovoltaic production capacity at the end of 2015 is estimated to be about 60 GW [1] and is expected to keep rising. Yet, there is great demand for increasing the photovoltaic device efficiency and cutting down the cost of materials, manufacturing, and installation. Materials and processing represent a large fraction of the expense. For example, material costs account for 40% of the total module price in the bulk crystalline silicon solar cells. Thin film solar cells have emerged as a means to reduce the material costs. To date, thin film solar cells are made

from various active inorganic materials, including amorphous and polycrystalline silicon, GaAs, $CuIn_xGa_{1-x}Se_2$ and CdTe, hybrid lead halide perovskites, as well as organic semiconductors. As the thickness of the absorbing semiconductor is decreased, the absorption naturally reduces at energies close to the band gap of the semiconductor. This is particularly a problem for thin film silicon solar cells. Thus, the compromise between enhancing the absorbance of broader solar lights and reducing the usage of narrower band gap semiconductor materials has to be taken in a thin film solar cell. And novel designs of thin film solar cells in which broadband light can be trapped inside to increase the absorption are highly needed to break the compromise balance.

In the past decade, a few light-trapping techniques have been investigated, among which a typical example is using a pyramidal surface texture [2]. However, such surface texture is intended for active light-harvesting layers, which are thicker than the wavelength of sunlight in the visible and near-infrared regions. The improved light trapping is balanced by the surface roughness that is almost the same order as the film thickness and by the increased surface recombination due to the larger surface area. Recently, the use of metallic nanostructures, which support surface plasmons (SPs) [3], has been regarded as an efficient way for enabling light trapping inside the active layer of a thin film solar cell and has consistently drawn an increasing amount of attention. SPs are coherent electron oscillations that propagate along the interface between a metal and a dielectric or semiconductor material. And SPs cause the electromagnetic field strongly confined at the metal/dielectric or semiconductor interface, with their intensity having an exponential dependence on the distance away from the interface. Thus near-field electromagnetic field enhancement and the enhanced scattering cross section (SCS) can be obtained through excitation of SPs. The larger electrical field means a stronger absorption, and a larger scattering cross section redirects more incident sunlight into the absorbing layer, resulting in a much larger light absorption in a much thinner semiconductor layer. Hence, both localized surface plasmons (LSPs) [4] excited in metallic nanoparticles and surface plasmon polaritons (SPPs) [5] propagating at the periodic metal/semiconductor interfaces have been so far widely investigated with great interests in designing high-efficient thin film solar cells [6–9].

In early work using plasmonic structures to improve the light absorption of photovoltaic devices, Au or Ag nanoparticles [5, 10] and nanograting [11] have been introduced into the front side of solar cells [5, 10–12]. Such efforts have common disadvantages that resonances can only occur at certain wavelengths, and the use of metallic nanostructures directly on top of solar cells will block a fairly large amount of total incident light. And then a layer of antireflection coating was combined into the surface metallic grating, to reduce the reflected light and thus to improve sunlight absorption [13]. The fractal-like pattern of Ag nano cuboids with several feature sizes [14] was employed to simultaneously excite low-index and high-index SP modes along the silicon-silver interface to achieve broadband absorption. On the other hand, Wang et al. [15] achieved a broadband and polarization-insensitive absorption enhancement by placing a metallic nanograting at the bottom of the optically active layer. In such design, planar waveguide modes, the Fabry-Pérot (FP) resonance, and the SPP resonance were effectively coupled, and photons blocking by the surface nanostructures can be avoided.

In Ref. [16], Ag nanocone was employed to enhance light trapping, and the simulated results showed that the normalized scattering cross section of the rear located Ag nanocone is higher than that of the front located one. Incorporation of embedded metal nanostructures for light trapping in thin film solar cell has been extensively investigated, such as, with nucleated silver nanoparticles embedded at rear side of amorphous silicon cells [17], using nanosphere [18], silver nanopillars [19], silver triangular [20], gold paired-strips [21] embedded grating structures, placing metal nanoparticles inside the active layer of solar cells [22], and with a metallic hole array inserted into a tandem solar cell [23]. Furthermore, combination of surface texture with embedded metal nanoparticles was also designed to trap light [24]. More plasmonic structures for light trapping in thin film solar cells will be described in the following sections in detail.

In this chapter, the theoretical formalisms about the SPPs and LSPs will be first described, followed by a summarize of plasmonic structures to improve the performance of thin film solar cell according to their positions of the nanostructures, which can be divided into at least three ways: (1) directly on top of thin film solar cell, (2) embedded at the bottom or middle of the optical absorber layer, and (3) combined with nanowire of optical absorber layer. Finally, conclusions are given.

2. Theory of surface plasmon

2.1. Surface plasmon polaritons

It has been more than a century since the electrons in solids were first regarded as hot dense plasma to explain some natural phenomenon like the color of metals and the temperature-dependent conductivity. Decades later since then, the word 'Plasmon' is carried out to describe a quantum of plasma oscillations, which are longitude density fluctuations that propagate through the volume of metal. The so-called volume plasmons have an eigen frequency $\omega_p = \sqrt{ne^2/m\varepsilon_0}$, when n is the electron density, at the order of 10 eV. They can be excited by both free electron beams and ultraviolet photons. In the 1950s, this was a fascinating phenomenon and has been well-studied theoretically and experimentally with electron-loss spectroscopy.

Probably as a result of the well investigations, in 1957, Rufus Ritchie [25] first predicted the existence of surface plasmons, which made up the other half of plasmon physics and is referred to as 'Plasmonics' nowadays. Surface plasmons are indeed the electron charges that perform coherent fluctuations on the metal boundary and are localized in the normal direction of the boundary within the Thomas-Fermi screening length. Polarized light source is frequently used to efficiently and conveniently excite a surface plasmon wave. Therefore, surface plasmon can also be treated as a collective set of surface plasmon polaritons (SPPs). Surface plasmon polariton is thus the elementary 'particle' of this unique surface phenomenon and will be investigated in the following.

Consider the simplest geometry sustaining SPPs, that is, a single and flat interface between a non-absorbing dielectric space with positive real dielectric constant ε_2 and a conductive space with complex dielectric function $\varepsilon_1(\omega)$. Maxwell's equations of macroscopic electromagnetism read:

$$\nabla \times \vec{E}\left(\vec{r},t\right) + \mu \frac{\partial \vec{H}\left(\vec{r},t\right)}{\partial t} = 0 \tag{1a}$$

$$\nabla \cdot \left(\mu \vec{H}\left(\vec{r},t\right)\right) = 0 \tag{1b}$$

$$\nabla \times \vec{H}\left(\vec{r},t\right) - \varepsilon_0 \varepsilon(\vec{r}) \frac{\partial \vec{E}\left(\vec{r},t\right)}{\partial t} = 0 \tag{1c}$$

$$\nabla \cdot \left(\varepsilon_0 \varepsilon(\vec{r}) \vec{E}\left(\vec{r},t\right)\right) = 0 \tag{1d}$$

There are two fundamental sets of solutions, which are termed as transverse magnetic (TM) and transverse electric (TE), respectively. Let us first look into TE solutions:

where $z > 0$:

$$E_y\left(z\right) = A_2 e^{i\beta x} e^{-k_2 z} \tag{2a}$$

$$H_x\left(z\right) = -iA_2 \frac{1}{\omega\mu_0} k_2 e^{i\beta x} e^{-k_2 z} \tag{2b}$$

$$H_z\left(z\right) = A_2 \frac{\beta}{\omega\mu_0} e^{i\beta x} e^{-k_2 z} \tag{2c}$$

And where $z < 0$:

$$E_y\left(z\right) = A_1 e^{i\beta x} e^{k_1 z} \tag{3a}$$

http://dx.doi.org/10.5772/65388

$$H_x(z) = iA_1 \frac{1}{\omega\mu_0} k_1 e^{i\beta x} e^{k_1 z} \tag{3b}$$

$$H_z(z) = A_1 \frac{\beta}{\omega\mu_0} e^{i\beta x} e^{k_1 z} \tag{3c}$$

Here the perpendicular component of wave vector $k_i(z)$ is denoted as k_i, with $i = 1, 2$ for short. Boundary condition requires the continuity of E_y and H_x at the interface $z = 0$, thus we have

$$A_1 = A_2 \tag{4a}$$

$$A_1(k_1 + k_2) = 0 \tag{4b}$$

Since k_i is positive, the only solution of Eq. (4) is $A_1 = A_2 = 0$. Hence, there are no possible surface modes for TE polarization. Now let us examine the result for TM polarization. Similarly, respective expressions for the field components in TM solutions are:

where $z > 0$:

$$H_y(z) = A_2 e^{i\beta x} e^{-k_2 z} \tag{5a}$$

$$E_x(z) = iA_2 \frac{1}{\omega\varepsilon_0\varepsilon_2} k_2 e^{i\beta x} e^{-k_2 z} \tag{5b}$$

$$E_z(z) = -A_2 \frac{\beta}{\omega\varepsilon_0\varepsilon_2} e^{i\beta x} e^{-k_2 z} \tag{5c}$$

and where $z < 0$:

$$H_y(z) = A_1 e^{i\beta x} e^{k_1 z} \tag{6a}$$

$$E_x(z) = -iA_1 \frac{1}{\omega\varepsilon_0\varepsilon_1} k_1 e^{i\beta x} e^{k_1 z} \tag{6b}$$

$$E_z(z) = -A_1 \frac{\beta}{\omega \varepsilon_0 \varepsilon_1} e^{i\beta x} e^{k_1 z} \tag{6c}$$

Boundary condition requires the continuity of H_y and $\varepsilon_i E_z$ at the interface $z = 0$, thus we have

$$A_1 = A_2 \tag{7a}$$

$$\frac{k_1}{k_2} = -\frac{\varepsilon_1}{\varepsilon_2} \tag{7b}$$

Different from the TE case, we can expect some non-null solution from Eq. (7). Note that the wave equation for TM modes reads:

$$\frac{\partial^2 H_y}{\partial z^2} + \left(k_0^2 \varepsilon - \beta^2\right) H_y = 0 \tag{8}$$

To fulfill Eq. (8) with the expression for H_y shown in Eqs. (5a) and (6a), we thus have

$$k_1^2 = \beta^2 - k_0^2 \varepsilon_1 \tag{9a}$$

$$k_2^2 = \beta^2 - k_0^2 \varepsilon_2 \tag{9b}$$

Combing this and Eq. (7), the solution at the boundary $z = 0$ is finally reached with propagating constant being:

$$\beta = k_0 \sqrt{\frac{\varepsilon_1 \varepsilon_2}{\varepsilon_1 + \varepsilon_2}} \tag{11}$$

Note that the metallic character of $\varepsilon_1(\omega)$ requires that ε_1 should be complex and its real part $\mathrm{Re}(\varepsilon_1) < 0$. Therefore, it is obvious that β is also complex, and its imaginary part indicates strong attenuation while propagating. By expanding $\varepsilon_1(\omega)$ into $\varepsilon_1' + i \cdot \varepsilon_1''$ and assuming $\left|\varepsilon_1'\right| \gg \varepsilon_1''$ as most metals do in reality, we further have

http://dx.doi.org/10.5772/65388

$$\beta = \beta' + i \cdot \beta'' = k_0 \sqrt{\frac{\varepsilon_1' \varepsilon_2}{\varepsilon_1' + \varepsilon_2}} + i k_0 \frac{\varepsilon_1''}{2\left(\varepsilon_1'\right)^2} \left(\frac{\varepsilon_1' \varepsilon_2}{\varepsilon_1' + \varepsilon_2} \right)^{3/2} \tag{12}$$

Here, β'' determines the attenuation of SPPs. On the other hand, one can say the reason for SPPs being surface mode is that SPPs will quickly vanish once it 'leaves' the surface. The energy is tightly bounded to the interface and travels only for a small amount of length, typically in the order of 1–10 wavelengths. This behavior is in nature similar to the well-known evanescence wave, and in fact, SPPs can be efficiently excited by the impact of evanescence wave when the momentum match between SPPs and the evanescent wave is satisfied. Unlike the old method using electron beam, optical way to excite SPPs is of much more convenience and efficiency and has paved the way for plasmonics into application.

2.2. Localized surface plasmons

If the interface supporting SPPs that we discussed above shrinks to the scale of nanometer and forms a closed surface like sphere or ellipsoid, there would be no SPPs existing as the dispersive relationship and boundary condition have changed. However, by simply assuming the electrons in such a tiny metal object to be a neutral plasma, one should expect that an intrinsic resonance similar to the volume plasma resonance still existed for it. In that case, electrons would also collectively oscillate with the impact photons. In fact, this behavior is reasonable and termed 'localized surface plasmon' (LSP). LSP should be in nature different from SPP because SPP can propagate along the interface while LSP is totally bounded and cannot propagate at all. In general, LSP does not consist of 'polaritons' as SPP does, hence we will call LSP directly in the following text.

Considering a metal sphere with radius R, which is much smaller than the incident light's wavelength, we could treat the incident electromagnetic field as a static electric field. Hence, under this static field approximation, the eigen modes for LSP can be solved from Laplace equations. The electrostatic potential from Laplace equations thus reads [26]:

$$\phi_{<}(r,\theta,\phi) = \sum_{l=0}^{\infty} \sum_{m=-l}^{l} a_{lm} r^l Y_{lm}(\theta,\phi) \tag{13a}$$

where $0 \le r \le R$ and

$$\phi_{>}(r,\theta,\phi) = \sum_{l=0}^{\infty} \sum_{m=-l}^{\infty} b_{lm} \frac{1}{r^{l+1}} Y_{lm}(\theta,\phi) \tag{13b}$$

Here $Y_{lm}(\theta,\phi)$ is the spherical harmonics, a_{lm} and b_{lm} are the coefficients. At the sphere surface, boundary condition requires φ and $\varepsilon \partial\varphi/\partial r$ to be continuous, thus we arrive at the dispersive relation for LSP:

$$\frac{\mathrm{Re}\,\varepsilon\left(\omega_{LSP}\right)}{\varepsilon_0}+\frac{l+1}{l}=0 \tag{14}$$

Assuming $\varepsilon(\omega_{LSP})$ has a Drude form, i.e., $\varepsilon\left(\omega_{LSP}\right)=1-\frac{\omega_p^2}{\omega^2}$ thus Eq. (14) turns into:

$$\omega_l=\omega_p\left[\frac{l}{\varepsilon_0\left(l+1\right)+l}\right] \tag{15}$$

where l stands for the angular momentum index. For a small enough sphere where the static field approximation is well satisfied, l thus equals to 1, which means that the dipole excitation is mainly responsible for LSP. With the increase in radius, the interaction between multipoles is becoming more and more important. Eventually at infinite radius, the frequency of LSP reaches that of SPPs at a semi-infinite metal-dielectric interface.

Similar to SPPs, LSPs exhibit an impressive local field enhancement as all energy is bounded. However, LSPs exist much more common than SPPs, as LSP does not require a specific polarization direction of the incident electromagnetic wave. A lot of applied techniques thus are developed on the basis of LSP enhancement, such as surface enhanced Raman spectroscopy (SERS), tip enhanced fluorescence spectroscopy (TEFS), and tip enhanced Raman spectroscopy (TERS).

3. Plasmonic light trapping in thin film solar cells

Metallic nanoparticles placed on the top of a solar cell will scatter the incident sunlight to couple and trap freely propagating plane waves into the active absorbing thin film, by folding the light into the thin film. When metallic nanoparticles are embedded inside of active layer, they can be treated as subwavelength antennas in which the plasmonic near-field is coupled to the absorbing layer, which will increase the effective absorption cross section. A patterned metallic structure on the backside of a thin absorber layer can couple sunlight into SPP modes, as well as the planar waveguide modes. Taking these light trapping effects into considerations, various structures have been designed to increase the light absorption of thin film solar cells.

3.1. Metallic nanostructures on top of thin film solar cell

When small metal nanoparticles are placed close to the surface of solar cell, light will mainly scatter into the dielectric with a larger permittivity [27]. The optical path length, thus, can be increased due to the scattered light obtains an angular spread in the dielectric. With a metallic reflector on the backside of the solar cell, the reflected light from the backside can couple to the surface nanoparticles and will reradiate into the active layer partly. In 2006, Yu et al. [12] deposited Au nanoparticles above the amorphous silicon film with thickness of only 240 nm.

They observed an 8.1% increase in short-circuit current density and an 8.3% increase in energy conversion efficiency with a modest density of Au particles. Moreover, finite-element electromagnetic simulations showed that substantially larger improvements should be attainable for higher nanoparticle densities. Ag nanoparticles were placed on top of a 1.25 μm thick Si-on-insulator solar cell; a broadband absorption enhancement and a 16-fold enhancement at 1050 nm were reported [10]. Atwater et al. [28] demonstrated that on GaAs thin cells with Ag nanoparticles located at the surface yielded a significant enhancement for wavelengths longer than 600 nm and exhibited an improvement of 8% for the short circuit current density. In addition, Au nanopillar [29] or Ag nanoparticle [30] was also used to excite the localized particle plasmon to enhance the light trapping in the organic solar cells, like P3HT: PCBM.

3.1.1. Effect of nanoparticle material, size, shape, and surrounding conditions

The surface nanoparticle material, size, shape, refractive index of the medium and distance from the active layer are key factors determining the scattering and coupling effect [6, 31–33]. In Ref. [33], the relationship between the normalized scattering cross section (SCS) and the spherical particle size in both air and silicon was investigated. The plasmonic resonance exhibits an obvious red-shift effect in Si compared to that in air. Additionally, the resonance peaks red shift and broaden with increasing particle size, which will significantly enhance the light trapping in the red and near-IR region. Typically, a relatively high scattering efficiency can be obtained with a particle size of ~100 nm. The particle shape also has effect on the efficiency. As shown in **Figure 1(a)**, cylindrical and hemispherical particles bring about much stronger light absorption enhancements than spherical particles [31], which may due to the fact that the average spacing to the substrate is smaller for these geometries than for spheres, and this allows efficient coupling of the scattered light into semiconductor substrates. The plasmon resonance peak always corresponds to the best light harvesting effect, and such resonance peak can be changed with the refractive index of the surrounding material. Plasmon resonances of Ag or Au nanoparticles locate at 350 and 480 nm, respectively, which can be red shifted over the entire 500–1500 nm by placing them in SiO_2, Si_3N_4, or Si [34–36]. When the distance between the nanoparticles and the absorbing layer increase, the light scattered into the absorbing layer will decrease [31]. However, such decrease is not significant. The carrier recombination occurs at the metal can be avoided due to separation by the dielectric layer. Moreover, increasing the distance between the nanoparticles and the absorbing layer can increase the SCS because large distance prevents destructive interference effects between the incident and reflected fields. Besides, it is demonstrated that Ag particles are better choice than Au, because Ag not only offers a lower price but also leads to much higher light absorption enhancement. Besides the noble metal, Al nanoparticles on front side of silicon solar cell show a 28.7% photon absorption enhancement in Si wafers, which is much larger than that induced by Ag or Au [37]. By combined with SiN_x anti-reflection coating, Al nanoparticles can even produce a 42.5% enhancement, which provides a low cost and high efficiency solution for practical larger-scale implementation of plasmonic nanoparticles for solar cell performance enhancement. Furthermore, it is experimentally demonstrated [38] that the use of periodic arrays of Al nanoparticles placed in the front of a thin Si film (shown in **Figure 1(b)**) causes a broadband photocurrent enhancement ranging from the ultraviolet to the infrared with respect

to the reference cell. Single particle resonances contribute to the enhancement in the infrared spectral range, and the collective resonances lead to an efficient coupling of light in the ultraviolet-blue range [38], thus a broadband enhancement can be realized.

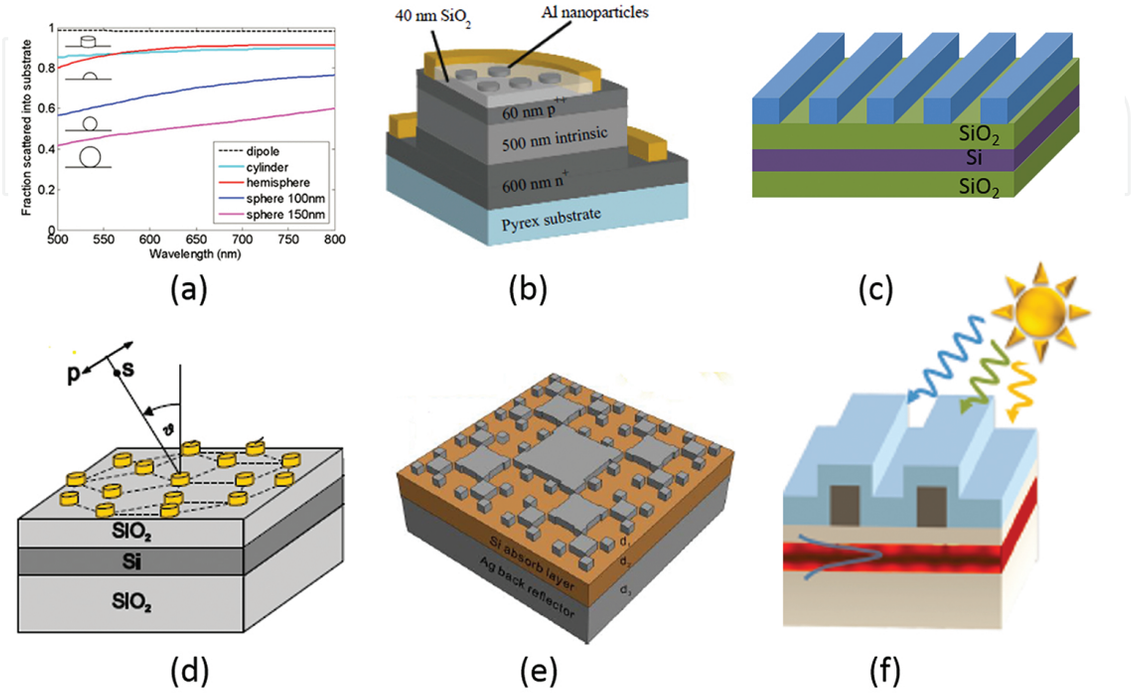

Figure 1. Various metallic nanostructures on top of thin film solar cells. (a) Fraction of light scattered into the substrate for different sizes and shapes of Ag particles on Si [31]; (b) Al nanoparticles placed on front of a thin Si film [38]; (c) Ag strips on the top of Si thin film cell [39]; (d) 2D quasiperiodic gold disks on top of the Si layer [43]; (e) a fractal-like pattern of silver nano cuboids on top of Si thin film cell [14]; (f) combination of AR coatings and gratings on top of ultrathin Si cell [44]. Figures reproduced with permission: (a) © 2008 AIP; (b) © 2015 OSA; (d), (e) © 2013 OSA; (f) © 2011 ACS.

3.1.2. Other surface nanostructures

In addition to metal nanoparticles, other structures such as gratings have also been employed for light trapping. Pala et al. [39] investigated the effect of periodic array of Ag strips (with the structure shown in **Figure 1(c)**) on the absorption enhancement in the Si thin film cell based on the finite-difference frequency-domain (FDFD) method. The simulation results show that the broadband light absorption benefits from the high near-fields surrounding the nanostructure and the effective coupling to waveguide supported by the thin Si film. Light absorption enhancement can be obtained both in the transverse electric (TE) and transverse magnetic (TM) polarized plane wave. For TM illumination, the Ag strips can effectively concentrate light in their vicinity at frequencies near their surface plasmon resonance, which depends on the strip geometry and its dielectric environment. And the sizes of Ag strips in the range from 50 to 100 nm are optimal. The lateral spacing of the strips governs the excitation of waveguide modes, while the number of allowed waveguide modes is determined by the thickness of the

Si layer. For TE illumination, only waveguide modes are excited, and the absorption enhancement directly results from an increased interaction length of the light with the Si film. Other structures like plasmonic cavity with subwavelength hole arrays [40] and nanotoroid arrays [41] were also employed in the P3HT: PCBM and silicon thin film solar cells, respectively.

3.1.3. Random nanostructures

Most plasmonic nanostructures designed on the front surface of thin film cells are always periodically distributed. Nishijima et al. [42] numerically and experimentally investigated the effect of periodic and random particle patterns on the plasmonic resonance. For the periodic arrays, the extinction peak (corresponding to the plasmonic resonance) value decreases with increasing periodicity, and the peak wavelength is red-shifted. The increasing disorder results in increasing extinction and a broader plasmon resonance, which may be due to grating-like diffraction losses. Light absorption is enhanced by more than two orders of magnitude for the random configuration of nanodiscs, demonstrated by the FDTD (finite-difference time-domain) simulations. The random structures applied to solar cell have advantages of simple and low-resolution fabrication. In Ref. [43], absorption enhancement by introducing 2D quasiperiodic and 2D periodic gold disks on top of the Si layer (with structure presented in **Figure 1(d)**) was compared. The simulation results present that, due to much more isotropic than the square lattice, the Penrose tiling structure can excite much more waveguide modes for absorbance spectra dependent on the azimuthal angle as well as the angle of incidence. Therefore, enhancement factor throughout the day as well as over the year may vary little. For the quasiperiodic lattice, the enhancement factor varies from 15.8 to 16.2 during summertime, whereas the variation ranges between 15.4 and 16.6 for the periodic lattice. Consequently, the performance of the solar cell with a quasicrystalline arrangement is expected to be more stable than that with a periodic one. An ultra-thin silicon solar cell coated by a fractal-like pattern of silver nanocuboids (as shown in **Figure 1(e)**) was investigated through FDTD simulation in Ref. [14], in which a broadband absorption is achieved due to the exists of multiple cavity modes and SP modes in the structure. The cavity modes come from Fabry-Pérot resonances at the longitudinal and transverse cavities, respectively. Low-index and high-index SP modes, which propagate along the silicon-silver interface, are simultaneously excited due to several feature sizes distributed in the fractal-like structure.

3.1.4. Combination of AR coating and metal nanostructures

Surface metal nanostructures have also been integrated with the antireflection (AR) coatings to enhance performance of plasmonic solar cells [44–46]. A detailed comparison between traditional AR coatings, plasmonic gratings, and structures that combine AR coatings and gratings on ultrathin Si absorbing layers (as shown in **Figure 1(f)**) was presented by FDTD simulations in Ref. [44]. Plasmonic gratings exhibit strong, narrow-band light absorption enhancement, while the traditional AR coatings result in more modest, broadband light absorption enhancement. The AR coatings even lead to stronger absorption than the gratings alone for the thicker films. However, the combination of AR coatings and gratings surpasses enhancements of either of these structures individually. The reason for this improvement

originates mainly from the enhanced absorption within the propagating periodic modes rather than the localized resonances for the structures. Al nanoparticles [45] located above a 75 nm silicon nitride antireflection coating in a 1 μm silicon film also provide a strong broadband light absorption enhancement.

3.2. Metallic nanostructures embedded inside the active layer

Designing the metallic nanostructures on top of solar cells has the problem of blocking a fairly large amount of total incident solar photons. While the metal nanostructures are placed at the bottom of optically active layer, they can be treated as back reflector and support SPP modes at the metal/semiconductor interface, as well as couple light into the photonic modes. Ferry et al. demonstrated [47] by numerical simulations that a single subwavelength scattering objects on the metallic back surface of a 200 nm Si thin film can enhance absorption by a factor of 2.5 over a large area for the portion of the solar spectrum near the Si band gap. The incident light is coupled into an SPP mode as well as a photonic mode that propagates inside the Si waveguide. And the coupling effect of each mode can be controlled by the height of the scatter. The photonic modes suffer from only very small losses in the metal. While for the ultrathin Si solar cell with thickness smaller than 100 nm, the photonic mode approaches its cutoff frequency and all the scattered light is converted into SPPs. The fraction of light coupled to both SPP and photonic modes increases with increasing wavelength because the incoming light at shorter wavelengths is directly absorbed in the Si layer.

Furthermore, Wang et al. [15] demonstrated that a broadband and polarization insensitive absorption enhancement was achieved in an α-Si cell with hybrid gratings of Ag and indium tin oxide (ITO) at the bottom of the a-Si layer (as presented in **Figure 2(a)**), which were originated from the effective coupling of planar waveguide modes, the Fabry-Pérot (FP) resonance and the SPP resonance. Similar to Ref. [47], the improvement mainly occurs at certain long wavelengths. The FP resonance inside the α-Si layer is excited both for TE or TM polarizations when both layer thickness and the incidence wavelength satisfy the resonance condition. Since the FP resonance is typically dependent on the thickness of α-Si layer, the added Ag nanograting will change the cavity thickness and cause the resonance red shift. Therefore, adjusting the Ag nanograting will be a practical means to tune the FP resonance to better fit the solar spectrum without changing the α-Si layer thickness. The excitation of guiding modes in the planar α-Si layer slab waveguide can lead to strong enhancement in the near-infrared regime for both TE and TE illuminations by adding the Ag nanograting. Such enhancement region red shifts with a thicker Si layer, a larger grating period, and a thicker Ag nanograting. The presence of the Ag nanograting provides more absorption enhancement for TM illumination, as SPPs are excited at both Si/Ag and ITO/Ag interfaces. Plasmonic wavelength is less dependent on α-Si thickness and red shifts as the grating's period increases. The absorption over the solar spectrum by such design shows an up to 30% broadband absorption enhancement when comparing to bare thin film cells, and the total enhancement under an unpolarized illumination varies little between 24 and 31% with an incident angle changing from 0 to 82°.

http://dx.doi.org/10.5772/65388

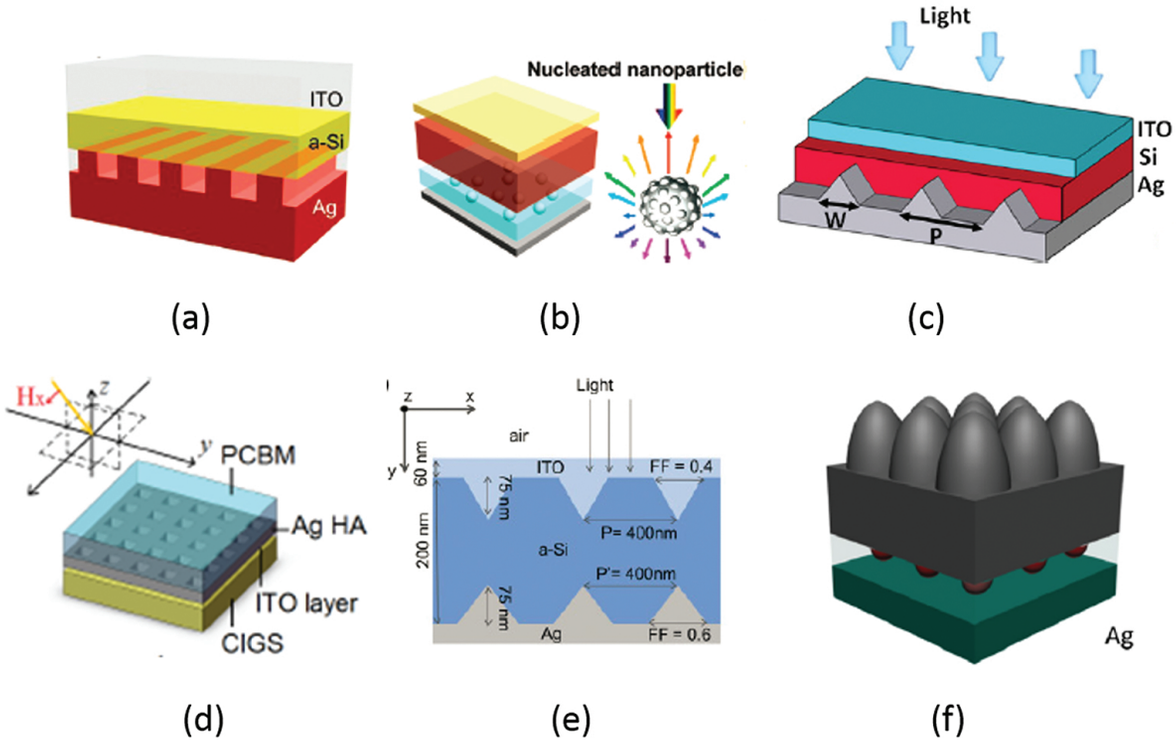

Figure 2. (a) Ag gratings at the bottom of thin film Si [15]; (b) nucleated Ag particles is embedded inside the ZnO layer at the rear side of the a-Si:H cell [17]; (c) Ag triangular corrugations at the bottom of a 100 nm c-Si cell [20]; (d) an Ag hole-array is inserted into a PCBM/CIGS tandem solar cell [53]; (e) Ag triangular gratings at the back side of cell and triangular ITO gratings at the front a-Si cell [65]; (f) the biomimetic silicon moth-eye structure combined with rear located Ag hemispherical particles in 2 μm thick c-Si cell [24]. Figures reproduced with permission: (a) © 2010 ACS; (b) © 2012 ACS; (c) © 2012 OSA; (d) © 2014 OSA; (e) © 2012 APS; (f) © 2016 OSA.

3.2.1. Various nanostructures at the bottom of active layer

Various plasmonic structures embedded at the back of active layer were proposed and investigated to enhance the solar cell absorption. Metal nanoparticles like nanospheres are widely employed [17–19, 48–50]. In Ref. [17], Chen et al. proposed a novel structure of glass/transparent conductive oxide (TCO)/p-i-n a-Si:H/ZnO:Ag, in which the nucleated Ag particles were embedded inside the ZnO layer at the rear side of the cell (as shown in **Figure 2(b)**). The simulations showed clearly that smaller nanoparticles (20–100 nm) have smaller scattering/absorption cross-sectional ratio but more equivalence in their scattering intensity versus angle distribution, while larger nanoparticles possess dominant scattering but focused primarily in limited scattering angles. Therefore, the proposed particle in Ref. [17] has a larger core with the surface simultaneously covered evenly with half-truncated small particles (1/5 size of the large particle). The larger particle brings about a larger scattering coefficient in the longer wavelength because of the excitation of the dipolar and quadrupolar plasmonic modes. And the smaller particle provides larger angle scattering for shorter wavelength light. The experimental results demonstrated that, compared with these of the randomly textured solar cells without nanoparticles, a broadband light absorption enhancement and prominent perform-

ance including a 23% improve of the energy conversion efficiency and a 14.3% increase in the short-circuit photocurrent density were achieved in the solar cells designed with 200 nm nucleated Ag nanoparticles with 10% coverage density. The surface coverage of the nucleated Ag particles at the rear side of cell should be set at the optimal range because too small coverage seems to be insufficient to cause significant light scattering, while too large may lead to obvious particle absorption.

In addition, an 80 nm thick Ag layer with triangular corrugations was designed on the bottom of a 100 nm thick c-Si layer, and the triangular corrugations (as shown in **Figure 2(c)**) were penetrated into the active Si layer [20]. Similar to Ref. [15], SPP mode and optical resonances contributed to the absorption enhancement. The FDTD simulation demonstrates that SPPs are excited at the Ag/Si interface of the triangular gratings, and the coupling of the excited SPP resonance with the FP resonance modes is observed for the TM illumination. For TE light, the excited cavity mode is demonstrated, and the coupling between waveguide and cavity modes is observed. Such triangular corrugations sustain large absorption enhancement factors (33.8–43.3%) up to relatively wide incidence angles, with enhancement higher than that using the Ag strip grating [15]. In Ref. [21], the FEM (finite element method) simulations demonstrated that the absorption enhancement with Au paired-strip grating embedded at back side of solar cell is higher than that with the Au single-strip grating. And the enhancement depends on the absorber layer thickness and the refractive index of the surrounding medium. Other structures like dual plasmonic nanostructures [51] are employed in single organic solar cells, in which Au nanoparticles are embedded in the active layer, and an Ag nanograting is used as the plasmonic back reflector. Through the collective excitation of Floquet modes, SPP, LSP, and their hybridizations, broadband absorption enhancement was observed both by experiment and simulation.

3.2.2. Metal nanostructures embedded in the middle of active layer

Absorption enhancement by plasmonic nanostructures embedded at the back side of active absorbing layer mainly focused on the long wavelength range, due to that the short wavelength part has mostly been absorbed by the solar cell. Therefore, plasmonic nanostructures embedded in the middle of the cell were also investigated [52–56]. Zhang et al. [53] proposed a structure that an Ag hole-array was inserted into a PCBM/CIGS tandem solar cell (as shown in **Figure 2(d)**). Such metallic hole array is expected to reflect the short-wavelength photons back to the top cell and transmit long-wavelength photons to the bottom cell through the extraordinary optical transmission (EOT) effect, as well as act as an intermediate electrode to allow a fabrication of hybrid organic-inorganic tandem solar cell. The simulation by FEM method demonstrates that for the cell including 100 nm PCBM/50 nm Ag hole-array/100 nm ITO/100 nm CIGS, the absorption inside the top subcell is always enhanced with different Ag hole array period, due to the back reflection of the Ag array, and for the bottom subcell, the absorption for the longer wavelength range (>650 nm) is greatly enhanced, originating from the EOT effect. When varying the period in the range from 200 nm to 1.5 μm, five resonant mechanisms are identified to participate in the EOT, including SPP mode, magnetic plasmon polaritons, LSP, and optical waveguide modes. It is shown that the thickness of Ag array or

that of ITO, the duty cycle of the holes also affects the optical performance of the cell. More than 40% integrated power enhancement can be achieved in a variable structural parameter range. Recently, metal nanoparticles are also placed at the middle of Si active layer [56] or the perovskite solar cell layer [55] to provide absorption enhancement.

3.2.3. Other effect in the embedded plasmonic nanostructure

Similar to plasmonic nanoparticles at the front side of solar cell, refractive index of the surrounding medium has effect on the plasmonic resonance and hence the absorption [57, 58]. Park et al. [57] applied the Ag nanoparticles on the rear side of p-Si tin film and investigated the optimum surface condition for plasmonic enhanced light absorption through experiment and simulation. It is found that the existence of SiO_2 layer between Si and Ag particles has a major effect on the SCS and hence the absorption in the cells. Peak of SCS with nanoparticles on the thermal SiO_2 is located at the light wavelengths <700 nm, while nanoparticles on the native SiO_2 layer and directly on Si show peaks of SCS at wavelengths >700 nm. The sample with nanoparticles on the native SiO_2 has the highest short-circuit current density enhancement. The simulation in Ref. [59] reveals that by tuning the thickness of Si and transparent conductive oxide layers in the ITO/a-Si:H/Ag nanoparticles/ZnO:Al/Ag mirror structure, the driving field intensity experienced by the embedded plasmonic particles can be enhanced up to a factor of 14. The effect of light losses induced by the rear located Ag nanoparticle on the light trapping of Si wafer was studied by Zhang et al. [60]. The light losses include the intrinsic absorption loss from Ag particles and the additional absorption loss induced by the void plasmons in the Al reflectors. The study reveals that Ag particles are effective to enhance the photocurrent in cells with planar front surface, while the absorption enhancement is substantially influenced by the plasmonics in the textured cells.

3.2.4. Comparison of plasmonic nanostructures located at different positions

Although the absorption enhancement can be achieved more or less by plasmonic nanostructure located at various positions of solar cell active layer, it is meaningful to compare the enhancement among the different locations of nanostructures [16, 61–64]. In early reports, metallic particle shapes such as spheres, hemispheres, and cylinders are commonly employed. It is usually seen that the SCS for the front located particles is obviously larger than that for the rear located particles when the dielectric spacer between metallic particles and absorbing layer is relatively thick [63, 64]. However, the front located particles involve a detrimental Fano effect resulting from the interference effects between the scattered light and the incident light, which reduces light absorption below the plasmon resonance wavelength. Using the rear located nanoparticles can avoid the Fano effect. Hence, the ideal design is to make the SCS value of the rear located particles higher than that of the front located particles for a wide range of the electric spacer thickness. Yan et al. [16] adopted an Ag nanocone as the plasmonic particles in the c-Si/Al_2O_3/Ag nanocone solar cell structure. The particles are treated as the front located particles when light is incident on the particles from air, while it is described as the rear ones if light is illuminated from the Si side. The FDTD simulation shows that the ratio of SCS between the rear and the front located particles at the resonance wavelength is near two

when the Al_2O_3 spacer thickness is 30 nm. And the ratio increases to three as the Al_2O_3 spacer thickness is 10 nm.

3.2.5. Combination of front and rear nanostructures

Dual-interface nanostructures [65–72] including the rear metal plasmonic grating/nanoparticles and the front dielectric grating or metal particles have also been adopted to enhance absorption efficiency in thin film solar cell. For example, in Ref. [65], an Ag triangular grating at the back side of cell and a triangular ITO grating at the front a-Si are combined (as shown in **Figure 2(e)**). The simulation presents that the ITO triangles focus on the short-wavelength incident light and subsequently spread it inside the active layer, and a combination of dielectric waveguide mode and FP resonance arises at 660 nm. Additionally, an absorption peak at 760 nm resulting from the waveguide mode and a peak at 810 nm corresponding to the plasmonic mode are observed. An integrated absorption for TM illumination of the AM 1.5 G spectrum in the 400–950 nm region is 83.1%. Having different periods at specific interfaces provides more efficient diffraction into both plasmonic and dielectric guide modes. Other similar structures like rear located Ag strip grating combined with silicon front surface trapezoidal [70] or strip [69] texture are reported too to enhance light trapping in Si thin film cell.

In Ref. [66], the Ag nanohemisphere is deposited on the rear of a nanohole-textured Si thin film. The role of Si nanohole is to absorb the light at the short wavelength, due to antireflection effect and light trapping properties. Long-wavelength light absorption benefits from the excitation of the LSP induced by the rear located Ag hemisphere. By adjusting parameters of Si nanohole and Ag hemisphere, the short-circuit current density can reach to 25.4 mA/cm^2. Shi et al. [71] combined silicon front surface grating and the rear-located bilayer Ag nanohemispheres. In that case, the grating and metal nanoparticles are optimized, and a short-circuit current density as high as 29.7 mA/cm^2 is obtained with a 1-μm thick c-Si cell. Similarly, Zhang et al. [24] propose a hybrid structure based on the biomimetic silicon moth-eye structure combined with rear located Ag hemispherical particles in the 2 μm thick c-Si cells (as shown in **Figure 2(f)**). The FDTD simulation results present the integrated light absorption enhancement over the solar spectrum is 69% compared with the cells with the conventional light trapping design, which is larger than these in only silicon moth-eye structure (58%) and only Ag hemisphere (41%). The photocurrent is as large as 33.4 mA/cm^2, which is higher than these in most structures.

3.3. Hybrid of metallic nanostructures with nanowire of optical absorber layer

Reducing the use of both active absorbing and non-earth abundant materials in thin film solar cell is pursued. A nanowire optical antenna absorber was proposed in Ref. [73], which demonstrated that the absorption of sunlight in Si nanowires can be significantly enhanced over the bulk Si. The active layer in the thin film solar cell structures was designed into nanostructures in quite a few researches [73–78], such as Si nanowire array with a wire-embedded Ag back reflector [76] and silicon nanocone hole solar cell with back located square Ag particle [78]. Wang et al. [75] patterned the entire $CuIn_xGa_{(1-x)}Se_2$ (CIGS) thin film cell into

an 1D nanograting array, with Ag strips on top of CIGS gratings and Ag planar acting as the surface and rear electrodes, respectively (as shown in **Figure 3(a)** and **(b)**). For TE illuminations, the observed larger absorption enhancement compared to the conventional cell mainly results from the scattering by the top electrode as well as the coupling with the multiple internal reflection resonance. As thickness of the CIGS layer increases, the light absorption enhancement shows a red shift and becomes broader and stronger simultaneously. In the case of TM light, SPPs are excited and lead to that most incoming light is transmitted through the Ag nanowire array. The transmitted light is confined in the CIGS wires, which results in a broadband absorption enhancement. Similar to the TE case, the SPP-related enhancement presents a red shift as the CIGS thickness increases. As the nanograting period and width increase, both magnitude and bandwidth of the enhancement first increase and then reduce beyond certain points. Such CIGS nanograting solar cell can enhance the overall current density over 250% compared to the bare thin film cells. In Ref. [77], the structure of Si nanowire/Si layer/ZnO:Al/Ag nanohemispheres back reflector (as shown in **Figure 3(c)**) is investigated through simulations. The nanohemispheres Ag back reflector can excite LSP resonance and cause scattering of light, giving rise to light absorption in Si. The short-circuit current density reaches to 28.4 mA/cm^2, demonstrating an enhancement of 22% compared with a Si nanowire solar cell with a planar back reflector.

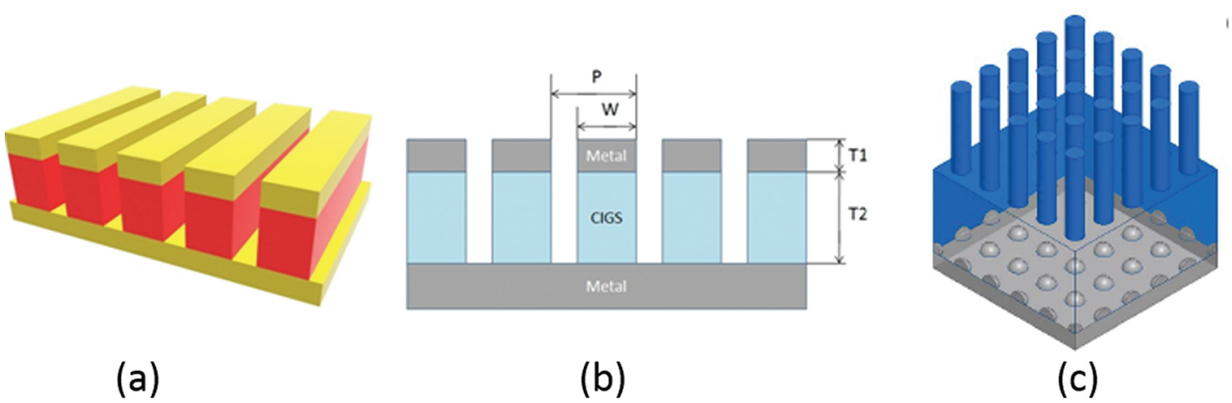

Figure 3. (a) The entire thin film cell $CuIn_xGa_{(1-x)}Se_2$(CIGS) is patterned into a 1D nanograting array, with Ag strips on top of CIGS gratings and Ag planar acting as surface and rear electrodes [75]; (b) cross-sectional view of (a); (c) Ag nanohemispheres at the bottom of Si nanowire cells [77]. Figures reproduced with permission: (a)–(c) © 2012 OSA.

4. Conclusions

In this chapter, we have summarized the advances in the research of light trapping and the plasmonic enhancement of thin film solar cells. Metallic nanoparticles can excite localized surface plasmons, which benefit for light scattering and light concentration to enhance the light absorption in thin film cell. A corrugated metallic film like grating on the absorber layer can couple sunlight into surface plasmon polaritons to enhance light absorption too. The light

enhancement by these plasmonic modes is strongly related to the material, size, shape, refractive index of the medium, position in the absorber layer of metallic nanoparticles, and metallic corrugated nanostructures.

The position of metal nanostructures has significant effect on the plasmonic solar cells. The metallic nanoparticles like hemispheres and cylinders on the front side of thin film solar cell have larger normalized scattering cross section than that for the rear located particles when the dielectric spacer between metallic particles and absorbing layer is relatively thick. However, the front located particles involve a detrimental Fano effect resulting from the interference effects between the scattered light and the incident light, which reduces light absorption below the plasmon resonance wavelength. The rear located nanoparticles can avoid such Fano effect. Therefore, careful designs like using rear located Ag nanocone can achieve larger SCS than that at front side. On the other hand, adopting the embedded metallic nanostructures can obtain broadband and polarization insensitive absorption enhancement benefiting from the effective coupling of planar waveguide modes, FP resonance and SPPs resonance. Furthermore, dual-interface hybrid structure based on the nanostructures of front surface absorber combined with rear located nanoparticles or nanograting may be an excellent way to enhance light absorption in thin film solar cells. Anyway, new plasmonic nanostructures still need to be investigated to further achieve broadband and polarization insensitive absorption enhancement at wide incident angles.

Acknowledgements

This work was supported by the National Basic Research Program of China (2012CB922000).

Author details

Qiuping Huang[1,3], Xiang Hu[1], Zhengping Fu[1] and Yalin Lu[1,2,3,4*]

*Address all correspondence to: yllu@ustc.edu.cn

1 Advanced Applied Research Center, Hefei National Laboratory for Physical Science at the Microscale, University of Science and Technology of China, Hefei, Anhui, PR China

2 National Synchrotron Radiation Laboratory, University of Science and Technology of China, Hefei, Anhui, PR China

3 Synergetic Innovation Center of Quantum Information & Quantum Physics, University of Science and Technology of China, Hefei, Hefei, PR China

4 Laser and Optics Research Center, Department of Physics, United States Air Force Academy, Colorado, USA

References

[1] International Technology Roadmap for Photovoltaic [Internet]. 2016. Available from: http://www.itrpv.net/Reports/Downloads/

[2] Green M. A. Lambertian light trapping in textured solar cells and light-emitting diodes: analytical solutions. Prog. Photovolt. 2002;10:235–41.

[3] Barnes W. L., Dereux A., Ebbesen T. W. Surface plasmon subwavelength optics. Nature. 2003;424:824–30.

[4] Rockstuhl C., Fahr S., Lederer F. Absorption enhancement in solar cells by localized plasmon polaritons. J. Appl. Phys. 2008;104:123102–7.

[5] Schaadt D. M., Feng B. , Yu E. T. Enhanced semiconductor optical absorption via surface plasmon excitation in metal nanoparticles. Appl. Phys. Lett. 2005;86:063106–3.

[6] Atwater H. A., Polman A. Plasmonics for improved photovoltaic devices. Nat. Mater. 2010;9:205–13.

[7] Spinelli P., Ferry V. E., Groep J., Lare M., Verschuuren M. A., Schropp R., Atwater H. A., Polman A. Plasmonic light trapping in thin-film Si solar cells. J. Opt. 2012;14:024002.

[8] Guo C., Sun T., Gao F., Liu Q., Ren Z. Metallic nanostructures for light trapping in energy-harvesting devices. Light Sci. Appl. 2014;3:e161.

[9] Tran H. N., Nguyen V. H., Nguyen B. H., Vu D. L. Light trapping and plasmonic enhancement in silicon, dye-sensitized and titania solar cells. Adv. Nat. Sci.: Nanosci. Nanotechnol. 2016;7:013001.

[10] Pillai S., Catchpole K. R., Trupke T., Green M. A. Surface plasmon enhanced silicon solar cells. J. Appl. Phys. 2007;101:093105–8.

[11] Pala R. A., White J., Barnard E., Liu J., Brongersma M. L. Design of plasmonic thin-film solar cells with broadband absorption enhancements. Adv. Mater. 2009;21:1–6.

[12] Derkacs D., Lim S. H., Matheu P., Mar W., Yu E. T. Improved performance of amorphous silicon solar cells via scattering from surface plasmon polaritons in nearby metallic nanoparticles. Appl. Phys. Lett. 2006;89:093103–3.

[13] Munday J. N., Atwater H. A. Large integrated absorption enhancement in plasmonic solar cells by combining metallic gratings and antireflection coatings. Nano Lett. 2010;11:2195–201.

[14] Zhu L., Shao M., Peng R., Fan R., Huang X., Wang M. Broadband absorption and efficiency enhancement of an ultra-thin silicon solar cell with a plasmonic fractal. Opt. Express. 2013;21:A313.

[15] Wang W., Wu S., Reinhardt K., Lu Y., Chen S. Broadband light absorption enhancement in thin-film silicon solar cells. Nano Lett. 2010;10:2012–18.

[16] Yan W., Stokes N., Jia B., and Gu M. Enhanced light trapping in the silicon substrate with plasmonic Ag nanocones. Opt. Lett. 2013;38:395.

[17] Chen X., Jia B., Saha J. K., Cai B., Stokes N., Qiao Q., Wang Y., Shi Z., Gu M. Broadband enhancement in thin-film amorphous silicon solar cells enabled by nucleated silver nanoparticles. Nano Lett. 2012;12:2187–92.

[18] Xu Q., Johnson C., Disney C., Pillai S. Enhanced broadband light trapping in c-Si solar cells using nanosphere-embedded metallic grating structure. IEEE J. Photovol. 2016;6:61–7.

[19] Mailhes R., Nychyporuk T., Lemiti M., Lysenko V. Plasmon-induced enhancement of optical absorption in silicon thin films due to embedded silver nano-pillars. Europhys. Lett. 2014;108:58005.

[20] Battal E., Yogurt T. A., Aygun L. E., Okyay A. K. Triangular metallic gratings for large absorption enhancement in thin film Si solar cells. Opt. Express. 2012;20:9458–64.

[21] Yang Z. Y. and Chen K. P. Effective absorption enhancement in dielectric thin-films with embedded paired-strips gold nanoantennas. Opt. Express. 2014;22:12737–49.

[22] Mopurisetty S. M., Bajaj M., Ganguly S. Beyond optical enhancement due to embedded metal nanoparticles in thin-film solar cells. Appl. Phys. Express. 2016;9:032301.

[23] Zhang X., Huang Q., Hu J., Knize R. J., Lu Y. Hybrid tandem solar cell enhanced by a metallic hole-array as the intermediate electrode. Opt. Express. 2014;22:A1400.

[24] Zhang Y., Jia B., Gu M. Biomimetic and plasmonic hybrid light trapping for highly efficient ultrathin crystalline silicon solar cells. Opt. Express. 2016;24:A506.

[25] Ritchie R. H. Plasma losses by fast electrons in thin films. Phys. Rev. 1957;106:874.

[26] Zayats A. V., Igor I. S., Alexei A. M. Nano-optics of surface plasmon polaritons. Phys. Rep. 2005;408:131–314.

[27] Mertz J. Radiative absorption, fluorescence, and scattering of a classical dipole near a lossless interface: a unified description. J. Opt. Soc. Am. B. 2000;17:1906.

[28] Nakayama K., Tanabe K., Atwater H. A. Plasmonic nanoparticle enhanced light absorption in GaAs solar cells. Appl. Phys. Lett. 2008;93:121904.

[29] Shu J. T., Mihaela B., Danilo B. R., Warren N. H., Huang C. K., Raymond J. P. Effect of gold nanopillar arrays on the absorption spectrum of a bulk heterojunction organic solar cell. Opt. Express. 2010;18:A528.

[30] Ren W., Zhang G., Wu Y., Ding H., Shen Q., Zhang K., et al. Broadband absorption enhancement achieved by optical layer mediated plasmonic solar cell. Opt. Express. 2011;19:26536.

[31] Catchpole K. R., Polman A. Design principles for particle plasmon enhanced solar cells. Appl. Phys. Lett. 2008;93:191113.

[32] Catchpole K. R., Polman A. Plasmonic solar cells. Opt. Express. 2008;16:21793–800.

[33] Pillai S., Green M. A. Plasmonics for photovoltaic applications. Sol. Energ. Mater. Sol. C Cells. 2010;94:1481–6.

[34] Beck F. J., Polman A., Catchpole K. R. Tunable light trapping for solar cells using localized surface plasmon. J. Appl. Phys. 2009;105:114310.

[35] Xu G., Tazawa M., Jin P., Nakao S., Yoshimura K.,Wavelength tuning of surface plasmon resonance using dielectric layers on silver island films. Appl. Phys. Lett. 2003;82:3811.

[36] Mertens H., Verhoeven J., Polman A., Tichelaar F. D. Infrared surface plasmons in two-dimensional silver nanoparticle arrays in silicon. Appl. Phys. Lett. 2004;85:1317.

[37] Zhang Y., Ouyang Z., Stokes N., Jia B., Shi Z., Gu M. Low cost and high performance Al nanoparticles for broadband light trapping in Si wafer solar cells. Appl. Phys. Lett. 2012;100:151101.

[38] Uhrenfeldt C., Villesen T. F., Tetu A., Johansen B., and Larsen A. N. Broadband photocurrent enhancement and light-trapping in thin film Si solar cells with periodic Al nanoparticle arrays on the front. Opt. Express. 2015;23:A525.

[39] Pala R. A., White J., Barnard E., Liu J., Brongersma M. L. Design of plasmonic thin-film solar cells with broadband absorption enhancements. Adv. Mater. 2009;21:3504–9.

[40] Chou S. Y., Ding W. Ultrathin, high-efficiency, broad-band, omni-acceptance, organic solar cells enhanced by plasmonic cavity with subwavelength hole array. Opt. Express. 2012;21:A60.

[41] Burford N., and Shenawee M. E. Optimization of silver nanotoroid arrays for the absorption enhancement of silicon thin-film solar cells. Plasmonics. 2015;10:225.

[42] Nishijima Y., Rosa L., Juodkazis S. Surface plasmon resonances in periodic and random patterns of gold nano-disks for broadband light harvesting. Opt. Express. 2012;20:11466.

[43] Bauer C., and Giessen H. Light harvesting enhancement in solar cells with quasicrystalline plasmonic structures. Opt. Express. 2013;21:A363.

[44] Munday J. N., and Atwater H. A. Large integrated absorption enhancement in plasmonic solar cells by combining metallic gratings and antireflection coatings. Nano Lett. 2011;11:2195.

[45] Zhang Y., Chen X., Ouyang Z., Lu H., Jia B., Shi Z., et al. Improved multicrystalline Si solar cells by light trapping from Al nanoparticle enhanced antireflection coating. Opt. Express. 2013;3:489.

[46] Juan F., Ramos C. C., Connolly J. P., David C., Abajo F. J., Hurtado J., et al. Effect of Ag nanoparticles integrated within antireflection coatings for solar cells. J. Renew. Sustain. Energy. 2013;5:033116.

[47] Ferry V. E., Sweatlock L. A., Pacifici D., Atwater H. A. Plasmonic nanostructure design for efficient light coupling into solar cells. Nano Lett. 2008;8:4391.

[48] Paetzold U. W., Moulin E., Michaelis D., Bottler W., Hagemann V., Meier M., et al. Plasmonic reflection grating back contacts for microcrystalline silicon solar cells. Appl. Phys. Lett. 2011;99:181105.

[49] Yang M., Li J., Lin F., Zhu X. Absorption enhancements in plasmonic solar cells coated with metallic nanoparticles. Plasmonics. 2013;8:877–83.

[50] Mizuno H., Sai H., Matsubara K., Takato H., Kondo M. Transfer-printed silver nanodisks for plasmonic light trapping in hydrogenated microcrystalline silicon solar cells. Appl. Phys. Express. 2014;7:112302.

[51] Li X., Choy W., Huo L., Xie F., Sha W., Ding B., et al. Dual plasmonic nanostructures for high performance inverted organic solar cells. Adv. Mater. 2012;24:3046–52.

[52] Wen L., Sun F., Chen Q. Cascading metallic gratings for broadband absorption enhancement in ultrathin plasmonic solar cells. Appl. Phys. Lett. 2014;104:151106.

[53] Zhang X., Huang Q., Hu J., Knize R., Lu Y. Hybrid tandem solar cell enhanced by a metallic hole-array as the intermediate electrode. Opt. Express. 2014;22:A1400.

[54] Liu L., Huo Y., Zhao K., Zhao T., Li Y. Broadband absorption enhancement in plasmonic thin-film solar cells with grating surface. Superlattices Microstruct. 2015;86:300–05.

[55] Yue L., Yan B., Attridge M., Wang Z. Light absorption in perovskite solar cell: fundamentals and plasmonic enhancement of infrared band absorption. Solar Energy. 2016;124:143–52.

[56] Mopurisetty S., Bajaj M., Ganguly S. Beyond optical enhancement due to embedded metal nanoparticles in thin-film solar cells. Appl. Phys. Express. 2016;9:032301.

[57] Park J., Park N., Varlamov S. Optimum surface condition for plasmonic Ag nanoparticles in polycrystalline silicon thin film solar cells. Appl. Phys. Lett. 2014;104:033903.

[58] Yang Y., Pillai S., Mehrvarz H., Kampwerth H., Baillie A., Green M. Enhanced light trapping for high efficiency crystalline solar cells by the application of rear surface plasmons. Sol. Energ. Mater. Sol. Cells. 2012;101:217.

[59] Santbergen R., Tan H., Zeman M., Smets A. Enhancing the driving field for plasmonic nanoparticles in thin-film solar cells. Opt. Express. 2014;22:A1023.

[60] Zhang Y., Jia B., Ouyang Z., Gu M. Influence of rear located silver nanoparticle induced light losses on the light trapping of silicon wafer-based solar cells. J. Appl. Phys. 2014;116:124303.

[61] Qu D., Liu F., Huang Y., Xie W., Xu Q. Mechanism of optical absorption enhancement in thin film organic solar cells with plasmonic metal nanoparticles. Opt. Express. 2011;19:24795.

[62] Winans J., Hungerford C., Shome K., Rothberg L., Fauchet P. Plasmonic effects in ultrathin amorphous silicon solar cells: performance improvements with Ag nanoparticles on the front, the back, and both. Opt. Express. 2015;23:A92.

[63] Beck F., Mollapati S., Polman A., Catchpole K. Asymmetry in photocurrent enhancement by plasmonic nanoparticle arrays located on the front or on the rear of solar cells. Appl. Phys. Lett. 2010;96:033113.

[64] Beck F., Verhagen E., Mokkapati S., Polman A., Catchpole K. Resonant SPP modes supported by discrete metal nanoparticles on high-index substrates. Opt. Express. 2011;19:A147.

[65] Abass A., Le K., Alu A., Burgelman M., Maes B. Dual-interface gratings for broadband absorption enhancement in thin-film solar cells. Phys. Rev. B. 2012;85:115449.

[66] Chen Y., Han W., Yang F. Enhanced optical absorption in nanohole-textured silicon thin-film solar cells with rear-located metal particles. Opt. Lett. 2013;38:3973.

[67] Zhang Y., Jia B., Gu M. Biomimetic and plasmonic hybrid light trapping for highly efficient ultrathin crystalline silicon solar cells. Opt. Express. 2016;24:A506.

[68] Li C., Xia L., Gao H., Shi R., Sun C., Shi H., et al. Broadband absorption enhancement in a-Si:H thin-film solar cells sandwiched by pyramidal nanostructured arrays. Opt. Express. 2012;20:A589.

[69] Chriki R., Yanai A., Shappir J., Levy U. Enhanced efficiency of thin film solar cells using a shifted dual grating plasmonic structure. Opt. Express. 2013;21:A382.

[70] Shi W., Fan R., Zhang K., Xu D., Xiong X., Peng R., et al. Broadband light trapping and absorption of thin-film silicon sandwiched by trapezoidal surface and silver grating. J. Appl. Phys. 2015;117:065104.

[71] Shi Y., Wang X., Liu W., Yang T., Ma J., Yang F. Extraordinary optical absorption based on diffraction grating and rear-located bilayer silver nanoparticles. Appl. Phys. Express. 2014;7:062301.

[72] Heidarzadeh H., Rostami A., Dolatyari M., Rostami G. Plasmon-enhanced performance of an ultrathinsilicon solar cell using metal-semiconductor core-shell hemispherical nanoparticles and metallic back grating. Appl. Opt. 2016;55:1779.

[73] Cao L., Fan P., Vasudev A., White J., Yu Z., Cai W., et al. Semiconductor nanowire optical antenna solar absorbers. Nano Lett. 2010;10:439.

[74] Mallick S., Agrawal M., Peumans P. Optimal light trapping in ultra-thin photonic crystal crystalline silicon solar cells. Opt. Express. 2010;18:5691.

[75] Wang W., Wu S., Knize R., Reinhardt K., Lu Y., Chen S. Enhanced photon absorption and carrier generation in nanowire solar cells. Opt. Express. 2012;20:3734.

[76] Zhou K., Guo Z., Li X., Jung J., Jee S, Park K., et al. The tradeoff between plasmonic enhancement and optical loss in silicon nanowire solar cells integrated in a metal back reflector. Opt. Express. 2012;20:A777.

[77] Ren R., Guo Y., Zhu R. Design of a plasmonic back reflector for silicon nanowire decorated solar cells. Opt. Lett. 2012;37:4245.

[78] Zhang X., Yu Y., Xi J., Liu T., Sun X. The plasmonic enhancement in silicon nanocone hole solar cells with back located metal particles. J. Opt. 2015;17:015901.